EUROPEAN ORGANIZATION FOR NUCLEAR RESEARCH (CERN)

CERN-EP-2021-188
LHCb-PAPER-2021-025
April 28, 2022

arXiv:2110.04497v2 [hep-ex] 27 Apr 2022

Observation of two new excited Ξ_b^0 states decaying to $\Lambda_b^0 K^- \pi^+$

LHCb collaboration[†]

Abstract

Two narrow resonant states are observed in the $\Lambda_b^0 K^- \pi^+$ mass spectrum using a data sample of proton-proton collisions at a center-of-mass energy of 13 TeV, collected by the LHCb experiment and corresponding to an integrated luminosity of $6\,\text{fb}^{-1}$. The minimal quark content of the $\Lambda_b^0 K^- \pi^+$ system indicates that these are excited Ξ_b^0 baryons. The masses of the $\Xi_b(6327)^0$ and $\Xi_b(6333)^0$ states are $m(\Xi_b(6327)^0) = 6327.28\,^{+0.23}_{-0.21} \pm 0.12 \pm 0.24\,\text{MeV}$ and $m(\Xi_b(6333)^0) = 6332.69\,^{+0.17}_{-0.18} \pm 0.03 \pm 0.22\,\text{MeV}$, respectively, with a mass splitting of $\Delta m = 5.41\,^{+0.26}_{-0.27} \pm 0.12\,\text{MeV}$, where the uncertainties are statistical, systematic and due to the Λ_b^0 mass measurement. The measured natural widths of these states are consistent with zero, with upper limits of $\Gamma(\Xi_b(6327)^0) < 2.20\ (2.56)\,\text{MeV}$ and $\Gamma(\Xi_b(6333)^0) < 1.60\ (1.92)\,\text{MeV}$ at a 90% (95%) credibility level. The significance of the two-peak hypothesis is larger than nine (five) Gaussian standard deviations compared to the no-peak (one-peak) hypothesis. The masses, widths and resonant structure of the new states are in good agreement with the expectations for a doublet of $1D$ Ξ_b^0 resonances.

Published in Phys. Rev. Lett. 128 (2022) 162001

© 2022 CERN for the benefit of the LHCb collaboration. CC BY 4.0 licence.

[†]Authors are listed at the end of this Letter.

In the constituent quark model [1,2], baryons comprising a b quark and two light quarks (bqq') form multiplets based on the symmetries of their flavor, spin, and spatial wave functions [3]. If q and q' are u or d quarks, these beauty baryons are classified into the Λ_b^0 and Σ_b baryon families, where the light diquark spin $j_{qq'}$ is 0 and 1, respectively. A beauty baryon containing one s quark (bsq) forms the Ξ_b or Ξ_b' family depending on whether the light diquark spin j_{sq} is 0 or 1. Most of the ground states of these beauty-baryon families have been observed [4]. Beyond that many radially and orbitally excited states with higher masses are predicted by theory [5–14]. In recent years, several excited Λ_b^0 states have been observed [15–17]. This motivates further investigations of the lesser known excited Ξ_b states, as the Λ_b^0 and Ξ_b states have similar properties due to the approximate $SU(3)$ flavor symmetry [5]. Recently, the LHCb collaboration reported the observation of the $\Xi_b(6227)^-$ baryon [18] and its isospin partner, the $\Xi_b(6227)^0$ baryon [19], and the CMS collaboration reported the observation of the $\Xi_b(6100)^-$ baryon [20]. No other excited Ξ_b states have been observed. There are predictions of two $1D$ Ξ_b^0 baryons mainly decaying through the $\Sigma_b^{(*)}K$ and $\Xi_b^{*,\prime}\pi$ modes [5, 9], where the label $1D$ refers to a unity radial quantum number and a D wave (orbital momentum $L = 2$) between the b quark and the light diquark system. A search for these predicted excited states and studies of their masses, widths and decay patterns can provide valuable validation to the understanding of quantum chromodynamics, which features the behavior of strong interactions. The $\Sigma_b^{(*)}K$ mode results in a $\Lambda_b^0 K^-\pi^+$ final state.

In this Letter, the observation of a structure with two narrow peaks in the $\Lambda_b^0 K^-\pi^+$ mass spectrum is presented (the inclusion of charge-conjugated processes is implied throughout this Letter), using proton-proton (pp) collision data collected by the LHCb experiment at a center-of-mass energy of $\sqrt{s} = 13\,\text{TeV}$, corresponding to an integrated luminosity of $6\,\text{fb}^{-1}$. A measurement of the mass and width of each state, and an investigation of the resonant structure contributing to the three-body decays of the excited Ξ_b^0 states are performed. The resulting properties are consistent with those predicted states for a $1D$ Ξ_b^0 doublet [5, 9], hereafter referred to as $\Xi_b(6327)^0$ and $\Xi_b(6333)^0$ states.

The LHCb detector [21, 22] is a single-arm forward spectrometer covering the pseudorapidity range $2 < \eta < 5$, designed for the study of particles containing b or c quarks. The detector includes a high-precision tracking system consisting of a silicon-strip vertex detector surrounding the pp interaction region [23], a large-area silicon-strip detector located upstream of a dipole magnet with a bending power of about 4 Tm, and three stations of silicon-strip detectors and straw drift tubes [24] placed downstream of the magnet. The tracking system provides a measurement of the momentum, p, of charged particles with a relative uncertainty that varies from 0.5% at low momentum to 1.0% at 200 GeV (natural units with $c = \hbar = 1$ are used throughout this Letter). The momentum scale of the tracking system is calibrated using samples of $J/\psi \to \mu^+\mu^-$ and $B^+ \to J/\psi K^+$ decays collected concurrently with the data sample used for this analysis [25, 26]. Different types of charged hadrons are distinguished using information from two ring-imaging Cherenkov detectors [27]. Photons, electrons and hadrons are identified by a calorimeter system consisting of scintillating-pad and preshower detectors, an electromagnetic and a hadronic calorimeter. Muons are identified by a system composed of alternating layers of iron and multiwire proportional chambers [28]. The online event selection is performed by a trigger [29, 30] which consists of a hardware stage, based on information from the calorimeter and muon systems, followed by a software stage, in which charged particles are reconstructed and a real-time analysis is performed. At the hardware stage, the pp

collision events are required to have a muon with high $p_{\rm T}$ or a hadron, photon or electron with large transverse energy deposited in the calorimeter. The software trigger requires a two-, three- or four-track secondary vertex with a significant displacement from any primary pp collision vertex (PV), and at least one charged particle with a large transverse momentum and inconsistent with originating from any PV. Simulation is required to model the effects of the detector acceptance, the imposed selection requirements and the detector resolution on the invariant mass spectrum. The pp collisions are generated using Pythia [31] with a specific LHCb configuration [32]. Decays of unstable particles are described by EvtGen [33], using Photos [34] and by the Geant4 toolkit [35, 36].

The Λ_b^0 baryon is reconstructed using its decays into the $\Lambda_c^+\pi^-$ and $\Lambda_c^+\pi^-\pi^+\pi^-$ final states, where the Λ_c^+ baryon subsequently decays to the $pK^-\pi^+$ final state. All charged final-state particles are required to have particle-identification information consistent with their respective mass hypotheses. A neural network is used to reject misreconstructed tracks [37]. To suppress combinatorial background from the PV, the final-state protons, kaons and pions are required to have transverse momenta $p_{\rm T} > 100\,{\rm MeV}$, $p > 1\,{\rm GeV}$ and $\chi^2_{\rm IP} > 4$ with respect to all PVs in the event, where $\chi^2_{\rm IP}$ of a particle is the difference in χ^2 of the vertex fit of a given PV, with the particle being included or excluded. The reconstructed Λ_c^+ vertex is required to have $\chi^2_{\rm vtx}/{\rm ndf} < 10$ and $\chi^2_{\rm FD} > 36$, where $\chi^2_{\rm vtx}$ is the χ^2 value of the vertex fit per degree of freedom, and $\chi^2_{\rm FD}$ is the χ^2 distance from the closest PV. The reconstructed mass must be within a window of $\pm 25\,{\rm MeV}$ ($\pm 18\,{\rm MeV}$) of the known Λ_c^+ mass [4] for $\Lambda_c^+\pi^-$ ($\Lambda_c^+\pi^-\pi^+\pi^-$) candidates. The tighter mass cut applied in the $\Lambda_c^+\pi^-\pi^+\pi^-$ sample is due to its higher background level. The selected Λ_c^+ candidates are further combined with pion candidates to form Λ_b^0 candidates, where the Λ_b^0 candidates are required to have $\chi^2_{\rm vtx}/{\rm ndf} < 10$ and a reconstructed proper lifetime larger than $0.2\,{\rm ps}$.

A boosted decision tree (BDT) algorithm [38–40] is used to enhance further the signal purity of the Λ_b^0 samples. The choice of the training variables follows similar strategies as that for $\Lambda_b^0 \to \Lambda_c^+\pi^-$ [16] and $\Lambda_b^0 \to \Lambda_c^+\pi^-\pi^+\pi^-$ [19] analysis. For both modes, the following variables are used: the $\chi^2_{\rm IP}$ values, the $p_{\rm T}$, and the $\chi^2_{\rm vtx}/{\rm ndf}$ of Λ_c^+ and Λ_b^0 candidates, the $\chi^2_{\rm FD}$, the angle between the reconstructed momentum and flight direction of the Λ_c^+ and Λ_b^0 candidates, and the quality of particle identification for final-state pions, kaons and protons. In addition, the $\chi^2_{\rm IP}$ value and $p_{\rm T}$ of the pion originating from the Λ_b^0 decay are used for the $\Lambda_b^0 \to \Lambda_c^+\pi^-$ mode, while the $\chi^2_{\rm IP}$ and flight-distance significance of the pion from the Λ_b^0 decay, the vertex-fit quality and the invariant mass of the $\pi^-\pi^+\pi^-$ system are used for the $\Lambda_b^0 \to \Lambda_c^+\pi^-\pi^+\pi^-$ mode. The BDT classifier is trained on data using background-subtracted [41] Λ_b^0 candidates to represent the signal sample, and Λ_b^0 candidates with $\Lambda_c^+\pi^-$ and $\Lambda_c^+\pi^-\pi^+\pi^-$ invariant mass ranging between 5700 and 5800 MeV (higher-mass sideband) to represent the background sample. Since the training samples are also used for the further analysis, the k-fold cross-validation technique [42] with $k = 10$ is applied to avoid any possible effect of overtraining. The chosen working point of the BDT classifier rejects half of the combinatorial background, with a negligible reduction on the signal efficiency. The resulting Λ_b^0 signal yields in the selected samples are 966 000 and 533 000 for the $\Lambda_b^0 \to \Lambda_c^+\pi^-$ and $\Lambda_b^0 \to \Lambda_c^+\pi^-\pi^+\pi^-$ decays, respectively. The invariant mass of selected $\Lambda_b^0 \to \Lambda_c^+\pi^-$ and $\Lambda_b^0 \to \Lambda_c^+\pi^-\pi^+\pi^-$ candidates is shown in the Supplemental Material of this Letter.

The selected Λ_b^0 candidates are further combined with a kaon and pion stemming from the pp interaction point to form the $\Lambda_b^0 K^-\pi^+$ candidates. The pion and kaon candidates are required to have $\chi^2_{\rm IP} < 9$, $\chi^2_{\rm trk}/{\rm ndf} < 3$ and to have $p > 1500\,{\rm MeV}$, $p_{\rm T}(K) >$

800 MeV, $p_{\rm T}(\pi) > 250$ MeV, where $\chi^2_{\rm trk}$/ndf is the track fit χ^2 per degree of freedom. Then Λ_b^0, pion and kaon are combined to form $\Lambda_b^0 K\pi$ candidates, which are required to have a vertex-fit χ^2 smaller than 20 and an invariant mass of the $\Lambda_b^0\pi$ system smaller than 5850 MeV. This is 10 MeV higher than the predicted kinematic maximum value of the $\Lambda_b^0\pi$ mass for the $\Xi_b(6327)^0$ and $\Xi_b(6333)^0$ states [5]. The $\Lambda_b^0 K^-\pi^+$ combinations containing the signal decays are hereafter referred to as the right-sign (RS) sample. For a better modeling of the background shape from random combinations of Λ_b^0, K^+ and π^- candidates, the wrong-sign (WS) candidates are reconstructed in the $\Lambda_b^0 K^+\pi^-$ final state. The same selections are applied to both the RS and WS samples. To improve the mass resolution of the excited Ξ_b^0 candidates, the reconstructed mass is redefined as $m(\Lambda_b^0 K\pi) \equiv M(\Lambda_b^0 K\pi) - M(\Lambda_c^+\pi^-(\pi^+\pi^-)) + M_{\Lambda_b^0}$, where $M_{\Lambda_b^0}$ is the known Λ_b^0 mass measured by the LHCb collaboration [43], $M(\Lambda_b^0 K\pi)$, $M(\Lambda_c^+\pi^-)$ and $M(\Lambda_c^+\pi^-\pi^+\pi^-)$ are the invariant masses calculated constraining [44] the Λ_c^+ mass to the world average value [4], and that the $\Lambda_b^0 K\pi$ and Λ_b^0 candidates originate in the PV.

The $m(\Lambda_b^0 K\pi)$ distributions of the RS and WS samples are shown in Fig. 1. Two narrow peaks can be seen around 6330 MeV in the $\Lambda_b^0 K^-\pi^+$ mass spectrum, while no significant peaking structure is visible in the $\Lambda_b^0 K^+\pi^-$ system. A simultaneous extended unbinned maximum-likelihood fit is performed to the RS and WS samples to determine the properties of the peaking structure. Each peak in the RS sample is modeled as a constant-width relativistic Breit–Wigner (RBW) function [45] defined as

$$f_{\rm sig}(m(\Lambda_b^0 K\pi)) = \frac{C_{\rm sig}}{(m^2 - m^2(\Lambda_b^0 K\pi))^2 + m^2\Gamma^2},$$

where $C_{\rm sig}$ is a normalization factor, m is the mass of Ξ_b^0 state, and Γ is its mass-independent width. The RBW function is convolved with a resolution model, parameterized as a symmetric variant of the Apollonios function [46]. The parameters of the resolution function are fixed to values determined from simulation. The background component, which is present in both the RS and WS samples, is described by a threshold function $f_{\rm bkg}(m(\Lambda_b^0 K\pi)) = C_{\rm bkg}(m(\Lambda_b^0 K\pi) - m_t)^{a_0} e^{-a_1(m(\Lambda_b^0 K\pi)-m_t)}$, where $C_{\rm bkg}$ is a normalization factor, a_0 and a_1 are free parameters in the fit, m_t is the minimum mass of the $\Lambda_b^0 K^-\pi^+$ combination, which corresponds to the sum of the Λ_b^0 [43], pion and kaon [4] masses. The same shape parameters for the background, a_0 and a_1, are shared by the RS and WS samples.

The masses and widths of the $\Xi_b(6327)^0$ and $\Xi_b(6333)^0$ states are measured to be

$$\begin{aligned}
m(\Xi_b(6327)^0) &= 6327.28^{+0.23}_{-0.21}\,\text{MeV},\\
m(\Xi_b(6333)^0) &= 6332.69^{+0.17}_{-0.18}\,\text{MeV},\\
\Gamma(\Xi_b(6327)^0) &= 0.93^{+0.74}_{-0.60}\,\text{MeV},\\
\Gamma(\Xi_b(6333)^0) &= 0.25^{+0.58}_{-0.25}\,\text{MeV},
\end{aligned}$$

with a mass splitting of $\Delta m \equiv m(\Xi_b(6333)^0) - m(\Xi_b(6327)^0) = 5.41^{+0.26}_{-0.27}$ MeV, and the resulting $\Xi_b(6327)^0$ and $\Xi_b(6333)^0$ signal yields are 134 ± 27 and 117 ± 24, respectively. The uncertainties listed above are statistical only.

A likelihood-ratio test statistic is used to estimate the global significance of the two observed states. For a first estimation based on Wilks' theorem [47], it is assumed that without these peaks, the value of twice the change of log-likelihood $\Delta_{2\log\mathcal{L}} \equiv 2\log(\mathcal{L}_{\rm max}/\mathcal{L}_0)$

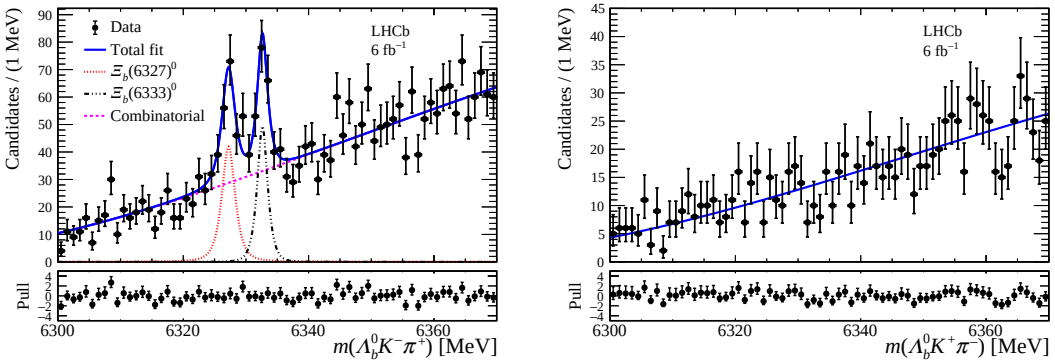

Figure 1: Invariant mass distributions of $\Lambda_b^0 K\pi$ candidates from (left) RS and (right) WS samples. The fit projections are overlaid. The black points with error bars correspond to the data, and the blue line shows the total fit projection. Individual fit components are listed in the legend.

follows a χ^2 distribution. The symbol $\mathcal{L}_{\rm max}$ indicates the maximum likelihood value with both peaks included in the fit model, while $\mathcal{L}_0$ is the value obtained from a null hypothesis with no peak or one peak included. The number of degrees of freedom of the χ^2 distribution is the difference of the number of floating parameters in the default fit and under the null hypothesis. With this method, the significance of the two-peak hypothesis is 10.4σ and 6.6σ with respect to the no-peak and one-peak hypotheses, respectively, where σ represents a Gaussian standard deviation. Pseudoexperiments are performed as an alternative method for estimating the statistical significance of the two-peak hypothesis with respect to the null hypothesis, including the no-peak and one-peak assumptions. A total of 200 000 pseudoexperiments are performed based on the null hypothesis and the $\Delta_{2\log\mathcal{L}}$ value is estimated for each of these. The $\Delta_{2\log\mathcal{L}}$ distribution is parameterized as a shape of which the tail can be modeled using a χ^2 distribution, with the number of degrees of freedom allowed to take non-integer values and determined by fitting the $\Delta_{2\log\mathcal{L}}$ distribution of the pseudoexperiments. When performing the pseudoexperiments, the look-elsewhere effect is considered by constraining the peaking position in several different mass intervals which combined together cover the full mass interval shown in Fig. 1. The p value of the two-peak hypothesis is estimated to be 10.2σ and 6.6σ, with no-peak and one-peak assumptions set as the null hypothesis, respectively. The significance from pseudoexperiments for the two hypotheses is consistent with the values from the Wilks' theorem [47], and the lowest values are taken as the statistical significance of the two observed states.

To study the resonant structure in the excited Ξ_b^0 decays, several $\Lambda_b^0 K^-\pi^+$ mass fits to data samples in 5 MeV wide slices of the $\Lambda_b^0\pi$ mass regions are performed. The default fit model described previously is used, with the masses and widths of the two Ξ_b^0 states fixed to the default values. The signal yields of $\Xi_b(6327)^0$ and $\Xi_b(6333)^0$ states as a function of the $\Lambda_b^0\pi$ mass are shown in Fig. 2, where significant peaking structure corresponding to the Σ_b^+ or Σ_b^{*+} states can be seen. The projections of the binned maximum-likelihood fits to the distributions are overlaid. The Σ_b^+ and Σ_b^{*+} contributions are modeled using a RBW amplitude with a mass-dependent width [45, 48], with the phase-space density of a three-body decay [4] and Blatt–Weisskopf barrier factors [48] considered when constructing the fit function. The non-resonant contribution (NR) is modeled using uniform-phase-space

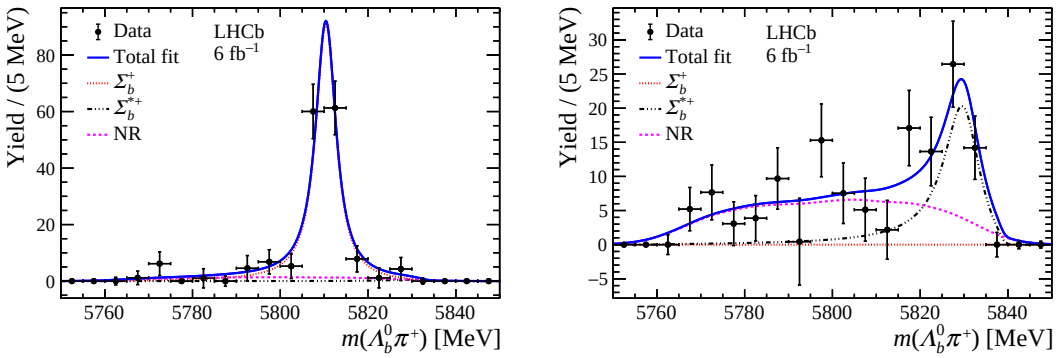

Figure 2: Signal yields of the (left) $\Xi_b(6327)^0$ and (right) $\Xi_b(6333)^0$ states determined by mass fits to data samples in 5 MeV slices of the $\Lambda_b^0\pi$ mass spectrum. The black points with error bars correspond to the yields of the $\Xi_b(6327)^0$ or $\Xi_b(6333)^0$ states, the blue solid lines are the total fit projections. Each individual component of the fit model is indicated in the legend.

simulation and obtained by a kernel estimation [49]. The interference between the NR component and the $\Sigma_b^{(*)+}$ resonances is not considered. The $\Xi_b(6327)^0$ state predominantly decays to $\Sigma_b^+K^-$. About half of the $\Xi_b(6333)^0$ baryons decay without $\Lambda_b^0\pi^+$ resonances, while the rest is dominated by the decay through the Σ_b^{*+} intermediate structure. The resonant structure is consistent with the theoretical predictions for a doublet of $1D$ Ξ_b^0 states [5, 9], where the $\Sigma_b^+K^-$ process dominates the decay of the lighter state, while the $\Sigma_b^{*+}K^-$ mode has a significant contribution to the decay of the heavier one.

Several sources of systematic uncertainties are considered for the mass and width measurements. The uncertainty related to the momentum scale is evaluated by varying the momentum scale within its known uncertainty of 3×10^{-4} [25, 26], and determining the effect on the mass and width parameters. To estimate the systematic uncertainties related to the choice of the functions used to model the signal and background shapes of the $\Lambda_b^0K\pi$ invariant mass spectra, several alternative fit models are used. The RBW functions with mass-dependent widths [45, 48] are used to model the Ξ_b^0 states, where the phase-space factors and barrier factors are calculated assuming the Ξ_b^0 decays to occur through the $\Xi_b^0 \to \Sigma_b^+K^-$ or $\Xi_b^0 \to \Sigma_b^{*+}K^-$ two-body processes. For these RBW functions, the orbital angular momentum of the $\Sigma_b^+K^-$ system is varied between 0 and 3 and the Blatt–Weisskopf barrier radius [48] between 1.0 and 5.0 GeV^{-1}. Polynomial functions with order between 2 and 4 are used as alternative models to describe the background and to estimate the corresponding systematic uncertainties. An alternative $\Lambda_b^0K\pi$ invariant-mass fit is performed using the default model but with only the RS sample, and the variation of the mass and width parameters are considered as the systematic uncertainties accounting for the potential discrepancy between the shapes of WS sample and RS background components. Alternative resolution functions, either the sum of two Crystal Ball [50] or of two Gaussian functions, are used to model the detector resolution effect. To consider the potential difference of mass resolution between data and simulation, the resolution determined by simulation is varied by $\pm 10\%$ [16, 18, 51–53] and the impact on the fit result is assigned as uncertainty. About 10% of the selected pp collision events contain more than one $\Lambda_b^0K^-\pi^+$ candidates, and these are retained in the data sample. As an alternative event-selection algorithm, only one candidate is kept for each event, and the variations of the mass and width parameters are treated as an additional source of

Table 1: Systematic uncertainties on masses and widths (in MeV) for the $\Xi_b(6327)^0$ and $\Xi_b(6333)^0$ states, and uncertainties from the Λ_b^0 mass measurement [43]. The systematic uncertainties due to the imperfect knowledge of the momentum scale (syst. momentum scale), systematic uncertainties from other sources (syst. excl. momentum scale), and the statistical uncertainties (stat.) are also listed as individual terms in this table.

Source	$\Xi_b(6327)^0$		$\Xi_b(6333)^0$		
	m	Γ	m	Γ	Δm
Momentum scale	0.06	0.06	0.03	0.04	0.03
Signal shape	0.01	0.12	0.00	0.25	0.01
Background shape	0.01	0.17	0.01	0.15	0.00
Resolution model	0.05	0.20	0.01	0.25	0.05
Multiple candidates	0.09	0.02	0.01	0.23	0.11
Total systematic uncertainty	0.12	0.30	0.03	0.45	0.12
Λ_b^0 mass (syst. momentum scale)	0.12	-	0.12	-	-
Λ_b^0 mass (syst. excl. momentum scale)	0.05	-	0.05	-	-
Λ_b^0 mass (stat.)	0.16	-	0.16	-	-
Total uncertainty from Λ_b^0 mass	0.24	-	0.22	-	-

systematic uncertainty. The significance of the two-peak structure is estimated based on all alternative fit models, and the smallest value is taken as the significance including systematic uncertainties. The significance of the two-peak structure is 9.9σ and 5.8σ with respect to the no-peak and one-peak hypotheses, respectively. As the reconstructed mass of the Ξ_b^0 candidates is defined using $M_{\Lambda_b^0}$ as an input, a corresponding uncertainty is considered. The value of $M_{\Lambda_b^0}$ is taken from the Λ_b^0 mass measurement performed by the LHCb collaboration [43], where the Λ_b^0 candidates are reconstructed with several Λ_b^0 decays excluding the $\Lambda_b^0 \to \Lambda_c^+\pi^-$ and $\Lambda_b^0 \to \Lambda_c^+\pi^-\pi^+\pi^-$ in this analysis. Therefore, the statistical uncertainty of the Λ_b^0 mass measurement is treated as an uncorrelated source of uncertainty. Among all sources of uncertainties of the Λ_b^0 mass result, only the systematic uncertainty related to the momentum scale is fully correlated with the corresponding uncertainty in this analysis, whereas the other systematic uncertainties are assumed to be uncorrelated. The total systematic uncertainty on the mass and width is calculated as the sum in quadrature of the different sources and summarized in Table 1.

The method to set an upper limit on the width is based on the Bayesian credibility level with a flat prior for non-negative width [4, 54]. The upper limits of the widths of the $\Xi_b(6327)^0$ and $\Xi_b(6333)^0$ states are evaluated by convolving the likelihood profiles with the total uncertainty of the width parameters in Table 1, and finding the values that cover 90% or 95% of the integrated probability.

In summary, two new states, $\Xi_b(6327)^0$ and $\Xi_b(6333)^0$, are observed in the $\Lambda_b^0 K^-\pi^+$ mass spectrum, where the Λ_b^0 baryon is reconstructed in the $\Lambda_c^+\pi^-$ and $\Lambda_c^+\pi^-\pi^+\pi^-$ final states. The significance of the two-peak hypothesis is larger than 9σ compared to the no-peak hypothesis and 5σ compared to the one-peak hypotheses in terms of Gaussian

standard deviations. The masses of these two states are measured to be

$$m(\Xi_b(6327)^0) = 6327.28\,^{+\,0.23}_{-\,0.21} \pm 0.12 \pm 0.24\,\text{MeV},$$
$$m(\Xi_b(6333)^0) = 6332.69\,^{+\,0.17}_{-\,0.18} \pm 0.03 \pm 0.22\,\text{MeV},$$

where the first uncertainties are statistical, the second systematic and the third is due to the Λ_b^0 mass measurement. The corresponding widths are consistent with zero, and upper limits at 90% (95%) credibility level are set,

$$\Gamma(\Xi_b(6327)^0) < 2.20\ (2.56)\,\text{MeV},$$
$$\Gamma(\Xi_b(6333)^0) < 1.60\ (1.92)\,\text{MeV}.$$

The mass differences between the excited Ξ_b^0 baryon and the ground state Λ_b^0 baryons are measured to be

$$m(\Xi_b(6327)^0) - M_{\Lambda_b^0} = 707.66\,^{+\,0.23}_{-\,0.21} \pm 0.12\,\text{MeV},$$
$$m(\Xi_b(6333)^0) - M_{\Lambda_b^0} = 713.07\,^{+\,0.17}_{-\,0.18} \pm 0.03\,\text{MeV},$$

with a mass splitting between the two Ξ_b^0 states of

$$\Delta m = 5.41\,^{+\,0.26}_{-\,0.27} \pm 0.12\,\text{MeV},$$

where the uncertainties are statistical and systematic, respectively. This is the first observation of two states decaying to the $\Lambda_b^0 K^- \pi^+$ final state. Their masses, widths and decay patterns are consistent with the predictions [5,9] for a doublet of $1D$ Ξ_b^0 states with $J^P = 3/2^+$ and $5/2^+$.

Acknowledgements

We express our gratitude to our colleagues in the CERN accelerator departments for the excellent performance of the LHC. We thank the technical and administrative staff at the LHCb institutes. We acknowledge support from CERN and from the national agencies: CAPES, CNPq, FAPERJ and FINEP (Brazil); MOST and NSFC (China); CNRS/IN2P3 (France); BMBF, DFG and MPG (Germany); INFN (Italy); NWO (Netherlands); MNiSW and NCN (Poland); MEN/IFA (Romania); MSHE (Russia); MICINN (Spain); SNSF and SER (Switzerland); NASU (Ukraine); STFC (United Kingdom); DOE NP and NSF (USA). We acknowledge the computing resources that are provided by CERN, IN2P3 (France), KIT and DESY (Germany), INFN (Italy), SURF (Netherlands), PIC (Spain), GridPP (United Kingdom), RRCKI and Yandex LLC (Russia), CSCS (Switzerland), IFIN-HH (Romania), CBPF (Brazil), PL-GRID (Poland) and NERSC (USA). We are indebted to the communities behind the multiple open-source software packages on which we depend. Individual groups or members have received support from ARC and ARDC (Australia); AvH Foundation (Germany); EPLANET, Marie Skłodowska-Curie Actions and ERC (European Union); A*MIDEX, ANR, IPhU and Labex P2IO, and Région Auvergne-Rhône-Alpes (France); Key Research Program of Frontier Sciences of CAS, CAS PIFI, CAS CCEPP, Fundamental Research Funds for the Central Universities, and Sci. & Tech. Program of Guangzhou (China); RFBR, RSF and Yandex LLC (Russia); GVA, XuntaGal and GENCAT (Spain); the Leverhulme Trust, the Royal Society and UKRI (United Kingdom).

Appendix: Supplemental material

The $\Lambda_b^0 \to \Lambda_c^+\pi^-$ and $\Lambda_b^0 \to \Lambda_c^+\pi^-\pi^+\pi^-$ candidates

The invariant mass of selected $\Lambda_b^0 \to \Lambda_c^+\pi^-$ and $\Lambda_b^0 \to \Lambda_c^+\pi^-\pi^+\pi^-$ candidates is shown in Fig. 3. To improve the Λ_b^0-candidate mass resolution, the Λ_b^0 mass is calculated by constraining the Λ_c^+ mass to its known value [4] and the Λ_b^0 baryon to originate from the associated PV [44]. Unbinned maximum-likelihood fits to the invariant mass distributions of the Λ_b^0 candidates are performed to estimate the Λ_b^0 signal yields. The signal component is described by the sum of a Gaussian function and two Crystal Ball functions [50] with the same mean value of the Gaussian cores and tail parameters determined from simulation. For the $\Lambda_b^0 \to \Lambda_c^+\pi^-$ mode, the background is described by misidentified $\Lambda_b^0 \to \Lambda_c^+K^-$ decays, the shape of which is determined from simulation, and combinatorial background modeled by an exponential function. For the $\Lambda_b^0 \to \Lambda_c^+\pi^-\pi^+\pi^-$ mode, only the combinatorial background, modeled by an exponential function, is considered. These fits are also shown in Fig. 3. The Λ_b^0 candidates are further required to have a reconstructed mass in a 2.5σ window around the value of the Λ_b^0 mass measured by the LHCb collaboration [43], where σ is the mass resolution of the data sample, determined to be 17.1 MeV for $\Lambda_b^0 \to \Lambda_c^+\pi^-$ and 13.9 MeV for $\Lambda_b^0 \to \Lambda_c^+\pi^-\pi^+\pi^-$ candidates.

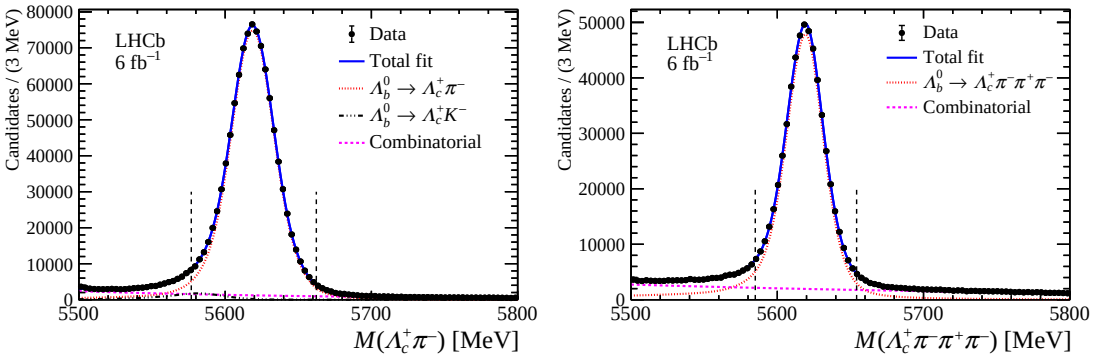

Figure 3: Invariant mass distributions of Λ_b^0 candidates reconstructed from (left) $\Lambda_b^0 \to \Lambda_c^+\pi^-$ and (right) $\Lambda_b^0 \to \Lambda_c^+\pi^-\pi^+\pi^-$ decays with fit projections overlaid. The black points with error bars correspond to the data, and the blue line shows the total fit projection. Individual fit components are listed in the legend. The Λ_b^0 candidates located between vertical dashed lines are used to form $\Lambda_b^0 K\pi$ combinations.

References

[1] M. Gell-Mann, *A schematic model of baryons and mesons*, Phys. Lett. **8** (1964) 214.

[2] G. Zweig, *An SU_3 model for strong interaction symmetry and its breaking; Version 1* CERN-TH-401, CERN, Geneva, 1964.

[3] E. Klempt and J.-M. Richard, *Baryon spectroscopy*, Rev. Mod. Phys. **82** (2010) 1095, arXiv:0901.2055.

[4] Particle Data Group, P. A. Zyla *et al.*, *Review of particle physics*, Prog. Theor. Exp. Phys. **2020** (2020) 083C01.

[5] B. Chen, S.-Q. Luo, X. Liu, and T. Matsuki, *Interpretation of the observed $\Lambda_b(6146)^0$ and $\Lambda_b(6152)^0$ states as 1D bottom baryons*, Phys. Rev. **D100** (2019) 094032, arXiv:1910.03318.

[6] B. Chen, K.-W. Wei, X. Liu, and A. Zhang, *Role of newly discovered $\Xi_b(6227)^-$ for constructing excited bottom baryon family*, Phys. Rev. **D98** (2018) 031502, arXiv:1805.10826.

[7] B. Chen and X. Liu, *Assigning the newly reported $\Sigma_b(6097)$ as a P-wave excited state and predicting its partners*, Phys. Rev. **D98** (2018) 074032, arXiv:1810.00389.

[8] D. Ebert, R. N. Faustov, and V. O. Galkin, *Spectroscopy and Regge trajectories of heavy baryons in the relativistic quark-diquark picture*, Phys. Rev. **D84** (2011) 014025, arXiv:1105.0583.

[9] Y.-X. Yao, K.-L. Wang, and X.-H. Zhong, *Strong and radiative decays of the low-lying D-wave singly heavy baryons*, Phys. Rev. **D98** (2018) 076015, arXiv:1803.00364.

[10] D. Ebert, R. N. Faustov, and V. O. Galkin, *Masses of excited heavy baryons in the relativistic quark model*, Phys. Lett. **B659** (2008) 612, arXiv:0705.2957.

[11] W. Roberts and M. Pervin, *Heavy baryons in a quark model*, Int. J. Mod. Phys. **A23** (2008) 2817, arXiv:0711.2492.

[12] B. Chen, K.-W. Wei, and A. Zhang, *Assignments of Λ_Q and Ξ_Q baryons in the heavy quark-light diquark picture*, Eur. Phys. J. **A51** (2015) 82, arXiv:1406.6561.

[13] K.-L. Wang, Y.-X. Yao, X.-H. Zhong, and Q. Zhao, *Strong and radiative decays of the low-lying S- and P-wave singly heavy baryons*, Phys. Rev. **D96** (2017) 116016, arXiv:1709.04268.

[14] Y. Kawakami and M. Harada, *Singly heavy baryons with chiral partner structure in a three-flavor chiral model*, Phys. Rev. **D99** (2019) 094016, arXiv:1902.06774.

[15] LHCb collaboration, R. Aaij *et al.*, *Observation of excited Λ_b^0 baryons*, Phys. Rev. Lett. **109** (2012) 172003, arXiv:1205.3452.

[16] LHCb collaboration, R. Aaij *et al.*, *Observation of new resonances in the $\Lambda_b^0\pi^+\pi^-$ system*, Phys. Rev. Lett. **123** (2019) 152001, arXiv:1907.13598.

[17] LHCb collaboration, R. Aaij *et al.*, *Observation of a new baryon state in the $\Lambda_b^0\pi^+\pi^-$ mass spectrum*, JHEP **06** (2020) 136, arXiv:2002.05112.

[18] LHCb collaboration, R. Aaij *et al.*, *Observation of a new Ξ_b^- resonance*, Phys. Rev. Lett. **121** (2018) 072002, arXiv:1805.09418.

[19] LHCb collaboration, R. Aaij *et al.*, *Observation of a new Ξ_b^0 state*, Phys. Rev. **D103** (2021) 012004, arXiv:2010.14485.

[20] CMS collaboration, A. M. Sirunyan *et al.*, *Observation of a new excited beauty strange baryon decaying to $\Xi_b^-\pi^+\pi^-$*, Phys. Rev. Lett. **126** (2021) 252003, arXiv:2102.04524.

[21] LHCb collaboration, A. A. Alves, Jr. *et al.*, *The LHCb detector at the LHC*, JINST **3** (2008) S08005.

[22] LHCb collaboration, R. Aaij *et al.*, *LHCb detector performance*, Int. J. Mod. Phys. **A30** (2015) 1530022, arXiv:1412.6352.

[23] R. Aaij *et al.*, *Performance of the LHCb Vertex Locator*, JINST **9** (2014) P09007, arXiv:1405.7808.

[24] R. Arink *et al.*, *Performance of the LHCb Outer Tracker*, JINST **9** (2014) P01002, arXiv:1311.3893.

[25] LHCb collaboration, R. Aaij *et al.*, *Measurements of the Λ_b^0, Ξ_b^-, and Ω_b^- baryon masses*, Phys. Rev. Lett. **110** (2013) 182001, arXiv:1302.1072.

[26] LHCb collaboration, R. Aaij *et al.*, *Precision measurement of D meson mass differences*, JHEP **06** (2013) 065, arXiv:1304.6865.

[27] M. Adinolfi *et al.*, *Performance of the LHCb RICH detector at the LHC*, Eur. Phys. J. **C73** (2013) 2431, arXiv:1211.6759.

[28] A. A. Alves Jr. *et al.*, *Performance of the LHCb muon system*, JINST **8** (2013) P02022, arXiv:1211.1346.

[29] R. Aaij *et al.*, *The LHCb trigger and its performance in 2011*, JINST **8** (2013) P04022, arXiv:1211.3055.

[30] R. Aaij *et al.*, *Design and performance of the LHCb trigger and full real-time reconstruction in Run 2 of the LHC*, JINST **14** (2019) P04013, arXiv:1812.10790.

[31] T. Sjöstrand, S. Mrenna, and P. Skands, *A brief introduction to PYTHIA 8.1*, Comput. Phys. Commun. **178** (2008) 852, arXiv:0710.3820.

[32] I. Belyaev *et al.*, *Handling of the generation of primary events in Gauss, the LHCb simulation framework*, J. Phys. Conf. Ser. **331** (2011) 032047.

[33] D. J. Lange, *The EvtGen particle decay simulation package*, Nucl. Instrum. Meth. **A462** (2001) 152.

[34] N. Davidson, T. Przedzinski, and Z. Was, *PHOTOS interface in C++: Technical and physics documentation*, Comp. Phys. Comm. **199** (2016) 86, arXiv:1011.0937.

[35] Geant4 collaboration, J. Allison *et al.*, *Geant4 developments and applications*, IEEE Trans. Nucl. Sci. **53** (2006) 270; Geant4 collaboration, S. Agostinelli *et al.*, *Geant4: A simulation toolkit*, Nucl. Instrum. Meth. **A506** (2003) 250.

[36] M. Clemencic *et al.*, *The LHCb simulation application, Gauss: Design, evolution and experience*, J. Phys. Conf. Ser. **331** (2011) 032023.

[37] M. De Cian, S. Farry, P. Seyfert, and S. Stahl, *Fast neural-net based fake track rejection in the LHCb reconstruction*, LHCb-PUB-2017-011, 2017.

[38] B. P. Roe *et al.*, *Boosted decision trees, an alternative to artificial neural networks*, Nucl. Instrum. Meth. **A543** (2005) 577, arXiv:physics/0408124.

[39] Y. Freund and R. E. Schapire, *A decision-theoretic generalization of on-line learning and an application to boosting*, J. Comput. Syst. Sci. **55** (1997) 119.

[40] H. Voss, A. Hoecker, J. Stelzer, and F. Tegenfeldt, *TMVA - Toolkit for Multivariate Data Analysis with ROOT*, PoS **ACAT** (2007) 040.

[41] M. Pivk and F. R. Le Diberder, *sPlot: A statistical tool to unfold data distributions*, Nucl. Instrum. Meth. **A555** (2005) 356, arXiv:physics/0402083.

[42] S. Geisser, *The predictive sample reuse method with applications*, Journal of the American Statistical Association **70** (1975) 320.

[43] LHCb collaboration, R. Aaij *et al.*, *Observation of the decays $\Lambda_b^0 \to \chi_{c1} p K^-$ and $\Lambda_b^0 \to \chi_{c2} p K^-$*, Phys. Rev. Lett. **119** (2017) 062001, arXiv:1704.07900.

[44] W. D. Hulsbergen, *Decay chain fitting with a Kalman filter*, Nucl. Instrum. Meth. **A552** (2005) 566, arXiv:physics/0503191.

[45] J. D. Jackson, *Remarks on the phenomenological analysis of resonances*, Nuovo Cim. **34** (1964) 1644.

[46] D. Martínez Santos and F. Dupertuis, *Mass distributions marginalized over per-event errors*, Nucl. Instrum. Meth. **A764** (2014) 150, arXiv:1312.5000.

[47] S. S. Wilks, *The large-sample distribution of the likelihood ratio for testing composite hypotheses*, Ann. Math. Stat. **9** (1938) 60.

[48] J. M. Blatt and V. F. Weisskopf, *Theoretical nuclear physics*, Springer, New York, 1952.

[49] K. S. Cranmer, *Kernel estimation in high-energy physics*, Comput. Phys. Commun. **136** (2001) 198, arXiv:hep-ex/0011057.

[50] T. Skwarnicki, *A study of the radiative cascade transitions between the Upsilon-prime and Upsilon resonances*, PhD thesis, Institute of Nuclear Physics, Krakow, 1986, DESY-F31-86-02.

[51] LHCb collaboration, R. Aaij *et al.*, *χ_{c1} and χ_{c2} resonance parameters with the decays $\chi_{c1,c2} \to J/\psi \mu^+ \mu^-$*, Phys. Rev. Lett. **119** (2017) 221801, arXiv:1709.04247.

[52] LHCb collaboration, R. Aaij *et al.*, *Observation of two new Ξ_b^- baryon resonances*, Phys. Rev. Lett. **114** (2015) 062004, arXiv:1411.4849.

[53] LHCb collaboration, R. Aaij *et al.*, *Near-threshold $D\overline{D}$ spectroscopy and observation of a new charmonium state*, JHEP **07** (2019) 035, arXiv:1903.12240.

[54] I. V. Narsky, *Estimation of upper limits using a Poisson statistic*, Nucl. Instrum. Meth. **A450** (2000) 444, arXiv:hep-ex/9904025.

LHCb collaboration

R. Aaij[32], A.S.W. Abdelmotteleb[56], C. Abellán Beteta[50], T. Ackernley[60], B. Adeva[46], M. Adinolfi[54], H. Afsharnia[9], C. Agapopoulou[13], C.A. Aidala[87], S. Aiola[25], Z. Ajaltouni[9], S. Akar[65], J. Albrecht[15], F. Alessio[48], M. Alexander[59], A. Alfonso Albero[45], Z. Aliouche[62], G. Alkhazov[38], P. Alvarez Cartelle[55], S. Amato[2], J.L. Amey[54], Y. Amhis[11], L. An[48], L. Anderlini[22], A. Andreianov[38], M. Andreotti[21], F. Archilli[17], A. Artamonov[44], M. Artuso[68], K. Arzymatov[42], E. Aslanides[10], M. Atzeni[50], B. Audurier[12], S. Bachmann[17], M. Bachmayer[49], J.J. Back[56], P. Baladron Rodriguez[46], V. Balagura[12], W. Baldini[21], J. Baptista Leite[1], M. Barbetti[22], R.J. Barlow[62], S. Barsuk[11], W. Barter[61], M. Bartolini[24,h], F. Baryshnikov[83], J.M. Basels[14], S. Bashir[34], G. Bassi[29], B. Batsukh[68], A. Battig[15], A. Bay[49], A. Beck[56], M. Becker[15], F. Bedeschi[29], I. Bediaga[1], A. Beiter[68], V. Belavin[42], S. Belin[27], V. Bellee[50], K. Belous[44], I. Belov[40], I. Belyaev[41], G. Bencivenni[23], E. Ben-Haim[13], A. Berezhnoy[40], R. Bernet[50], D. Berninghoff[17], H.C. Bernstein[68], C. Bertella[48], A. Bertolin[28], C. Betancourt[50], F. Betti[48], Ia. Bezshyiko[50], S. Bhasin[54], J. Bhom[35], L. Bian[73], M.S. Bieker[15], S. Bifani[53], P. Billoir[13], M. Birch[61], F.C.R. Bishop[55], A. Bitadze[62], A. Bizzeti[22,k], M. Bjørn[63], M.P. Blago[48], T. Blake[56], F. Blanc[49], S. Blusk[68], D. Bobulska[59], J.A. Boelhauve[15], O. Boente Garcia[46], T. Boettcher[65], A. Boldyrev[82], A. Bondar[43], N. Bondar[38,48], S. Borghi[62], M. Borisyak[42], M. Borsato[17], J.T. Borsuk[35], S.A. Bouchiba[49], T.J.V. Bowcock[60], A. Boyer[48], C. Bozzi[21], M.J. Bradley[61], S. Braun[66], A. Brea Rodriguez[46], M. Brodski[48], J. Brodzicka[35], A. Brossa Gonzalo[56], D. Brundu[27], A. Buonaura[50], L. Buonincontri[28], A.T. Burke[62], C. Burr[48], A. Bursche[72], A. Butkevich[39], J.S. Butter[32], J. Buytaert[48], W. Byczynski[48], S. Cadeddu[27], H. Cai[73], R. Calabrese[21,f], L. Calefice[15,13], L. Calero Diaz[23], S. Cali[23], R. Calladine[53], M. Calvi[26,j], M. Calvo Gomez[85], P. Camargo Magalhaes[54], P. Campana[23], A.F. Campoverde Quezada[6], S. Capelli[26,j], L. Capriotti[20,d], A. Carbone[20,d], G. Carboni[31], R. Cardinale[24,h], A. Cardini[27], I. Carli[4], P. Carniti[26,j], L. Carus[14], K. Carvalho Akiba[32], A. Casais Vidal[46], G. Casse[60], M. Cattaneo[48], G. Cavallero[48], S. Celani[49], J. Cerasoli[10], D. Cervenkov[63], A.J. Chadwick[60], M.G. Chapman[54], M. Charles[13], Ph. Charpentier[48], G. Chatzikonstantinidis[53], C.A. Chavez Barajas[60], M. Chefdeville[8], C. Chen[3], S. Chen[4], A. Chernov[35], V. Chobanova[46], S. Cholak[49], M. Chrzaszcz[35], A. Chubykin[38], V. Chulikov[38], P. Ciambrone[23], M.F. Cicala[56], X. Cid Vidal[46], G. Ciezarek[48], P.E.L. Clarke[58], M. Clemencic[48], H.V. Cliff[55], J. Closier[48], J.L. Cobbledick[62], V. Coco[48], J.A.B. Coelho[11], J. Cogan[10], E. Cogneras[9], L. Cojocariu[37], P. Collins[48], T. Colombo[48], L. Congedo[19,c], A. Contu[27], N. Cooke[53], G. Coombs[59], I. Corredoira [46], G. Corti[48], C.M. Costa Sobral[56], B. Couturier[48], D.C. Craik[64], J. Crkovská[67], M. Cruz Torres[1], R. Currie[58], C.L. Da Silva[67], S. Dadabaev[83], L. Dai[71], E. Dall'Occo[15], J. Dalseno[46], C. D'Ambrosio[48], A. Danilina[41], P. d'Argent[48], J.E. Davies[62], A. Davis[62], O. De Aguiar Francisco[62], K. De Bruyn[79], S. De Capua[62], M. De Cian[49], J.M. De Miranda[1], L. De Paula[2], M. De Serio[19,c], D. De Simone[50], P. De Simone[23], J.A. de Vries[80], C.T. Dean[67], D. Decamp[8], V. Dedu[10], L. Del Buono[13], B. Delaney[55], H.-P. Dembinski[15], A. Dendek[34], V. Denysenko[50], D. Derkach[82], O. Deschamps[9], F. Desse[11], F. Dettori[27,e], B. Dey[77], A. Di Cicco[23], P. Di Nezza[23], S. Didenko[83], L. Dieste Maronas[46], H. Dijkstra[48], V. Dobishuk[52], C. Dong[3], A.M. Donohoe[18], F. Dordei[27], A.C. dos Reis[1], L. Douglas[59], A. Dovbnya[51], A.G. Downes[8], M.W. Dudek[35], L. Dufour[48], V. Duk[78], P. Durante[48], J.M. Durham[67], D. Dutta[62], A. Dziurda[35], A. Dzyuba[38], S. Easo[57], U. Egede[69], V. Egorychev[41], S. Eidelman[43,v], S. Eisenhardt[58], S. Ek-In[49], L. Eklund[59,86], S. Ely[68], A. Ene[37], E. Epple[67], S. Escher[14], J. Eschle[50], S. Esen[13], T. Evans[48], A. Falabella[20], J. Fan[3], Y. Fan[6], B. Fang[73], S. Farry[60], D. Fazzini[26,j], M. Féo[48], A. Fernandez Prieto[46], A.D. Fernez[66], F. Ferrari[20,d], L. Ferreira Lopes[49], F. Ferreira Rodrigues[2], S. Ferreres Sole[32], M. Ferrillo[50], M. Ferro-Luzzi[48], S. Filippov[39], R.A. Fini[19], M. Fiorini[21,f], M. Firlej[34], K.M. Fischer[63], D.S. Fitzgerald[87], C. Fitzpatrick[62], T. Fiutowski[34], A. Fkiaras[48], F. Fleuret[12],

M. Fontana[13], F. Fontanelli[24,h], R. Forty[48], D. Foulds-Holt[55], V. Franco Lima[60], M. Franco Sevilla[66], M. Frank[48], E. Franzoso[21], G. Frau[17], C. Frei[48], D.A. Friday[59], J. Fu[6], Q. Fuehring[15], E. Gabriel[32], A. Gallas Torreira[46], D. Galli[20,d], S. Gambetta[58,48], Y. Gan[3], M. Gandelman[2], P. Gandini[25], Y. Gao[5], M. Garau[27], L.M. Garcia Martin[56], P. Garcia Moreno[45], J. García Pardiñas[26,j], B. Garcia Plana[46], F.A. Garcia Rosales[12], L. Garrido[45], C. Gaspar[48], R.E. Geertsema[32], D. Gerick[17], L.L. Gerken[15], E. Gersabeck[62], M. Gersabeck[62], T. Gershon[56], D. Gerstel[10], Ph. Ghez[8], L. Giambastiani[28], V. Gibson[55], H.K. Giemza[36], A.L. Gilman[63], M. Giovannetti[23,p], A. Gioventù[46], P. Gironella Gironell[45], L. Giubega[37], C. Giugliano[21,f,48], K. Gizdov[58], E.L. Gkougkousis[48], V.V. Gligorov[13], C. Göbel[70], E. Golobardes[85], D. Golubkov[41], A. Golutvin[61,83], A. Gomes[1,a], S. Gomez Fernandez[45], F. Goncalves Abrantes[63], M. Goncerz[35], G. Gong[3], P. Gorbounov[41], I.V. Gorelov[40], C. Gotti[26], E. Govorkova[48], J.P. Grabowski[17], T. Grammatico[13], L.A. Granado Cardoso[48], E. Graugés[45], E. Graverini[49], G. Graziani[22], A. Grecu[37], L.M. Greeven[32], N.A. Grieser[4], L. Grillo[62], S. Gromov[83], B.R. Gruberg Cazon[63], C. Gu[3], M. Guarise[21], M. Guittiere[11], P. A. Günther[17], E. Gushchin[39], A. Guth[14], Y. Guz[44], T. Gys[48], T. Hadavizadeh[69], G. Haefeli[49], C. Haen[48], J. Haimberger[48], T. Halewood-leagas[60], P.M. Hamilton[66], J.P. Hammerich[60], Q. Han[7], X. Han[17], T.H. Hancock[63], S. Hansmann-Menzemer[17], N. Harnew[63], T. Harrison[60], C. Hasse[48], M. Hatch[48], J. He[6,b], M. Hecker[61], K. Heijhoff[32], K. Heinicke[15], A.M. Hennequin[48], K. Hennessy[60], L. Henry[48], J. Heuel[14], A. Hicheur[2], D. Hill[49], M. Hilton[62], S.E. Hollitt[15], R. Hou[7], Y. Hou[6], J. Hu[17], J. Hu[72], W. Hu[7], X. Hu[3], W. Huang[6], X. Huang[73], W. Hulsbergen[32], R.J. Hunter[56], M. Hushchyn[82], D. Hutchcroft[60], D. Hynds[32], P. Ibis[15], M. Idzik[34], D. Ilin[38], P. Ilten[65], A. Inglessi[38], A. Ishteev[83], K. Ivshin[38], R. Jacobsson[48], H. Jage[14], S. Jakobsen[48], E. Jans[32], B.K. Jashal[47], A. Jawahery[66], V. Jevtic[15], F. Jiang[3], M. John[63], D. Johnson[48], C.R. Jones[55], T.P. Jones[56], B. Jost[48], N. Jurik[48], S.H. Kalavan Kadavath[34], S. Kandybei[51], Y. Kang[3], M. Karacson[48], M. Karpov[82], F. Keizer[48], D.M. Keller[68], M. Kenzie[56], T. Ketel[33], B. Khanji[15], A. Kharisova[84], S. Kholodenko[44], T. Kirn[14], V.S. Kirsebom[49], O. Kitouni[64], S. Klaver[32], N. Kleijne[29], K. Klimaszewski[36], M.R. Kmiec[36], S. Koliiev[52], A. Kondybayeva[83], A. Konoplyannikov[41], P. Kopciewicz[34], R. Kopecna[17], P. Koppenburg[32], M. Korolev[40], I. Kostiuk[32,52], O. Kot[52], S. Kotriakhova[21,38], P. Kravchenko[38], L. Kravchuk[39], R.D. Krawczyk[48], M. Kreps[56], F. Kress[61], S. Kretzschmar[14], P. Krokovny[43,v], W. Krupa[34], W. Krzemien[36], W. Kucewicz[35,t], M. Kucharczyk[35], V. Kudryavtsev[43,v], H.S. Kuindersma[32,33], G.J. Kunde[67], T. Kvaratskheliya[41], D. Lacarrere[48], G. Lafferty[62], A. Lai[27], A. Lampis[27], D. Lancierini[50], J.J. Lane[62], R. Lane[54], G. Lanfranchi[23], C. Langenbruch[14], J. Langer[15], O. Lantwin[83], T. Latham[56], F. Lazzari[29,q], R. Le Gac[10], S.H. Lee[87], R. Lefèvre[9], A. Leflat[40], S. Legotin[83], O. Leroy[10], T. Lesiak[35], B. Leverington[17], H. Li[72], P. Li[17], S. Li[7], Y. Li[4], Y. Li[4], Z. Li[68], X. Liang[68], T. Lin[61], R. Lindner[48], V. Lisovskyi[15], R. Litvinov[27], G. Liu[72], H. Liu[6], Q. Liu[6], S. Liu[4], A. Lobo Salvia[45], A. Loi[27], J. Lomba Castro[46], I. Longstaff[59], J.H. Lopes[2], S. Lopez Solino[46], G.H. Lovell[55], Y. Lu[4], C. Lucarelli[22], D. Lucchesi[28,l], S. Luchuk[39], M. Lucio Martinez[32], V. Lukashenko[32,52], Y. Luo[3], A. Lupato[62], E. Luppi[21,f], O. Lupton[56], A. Lusiani[29,m], X. Lyu[6], L. Ma[4], R. Ma[6], S. Maccolini[20,d], F. Machefert[11], F. Maciuc[37], V. Macko[49], P. Mackowiak[15], S. Maddrell-Mander[54], O. Madejczyk[34], L.R. Madhan Mohan[54], O. Maev[38], A. Maevskiy[82], D. Maisuzenko[38], M.W. Majewski[34], J.J. Malczewski[35], S. Malde[63], B. Malecki[48], A. Malinin[81], T. Maltsev[43,v], H. Malygina[17], G. Manca[27,e], G. Mancinelli[10], D. Manuzzi[20,d], D. Marangotto[25,i], J. Maratas[9,s], J.F. Marchand[8], U. Marconi[20], S. Mariani[22,g], C. Marin Benito[48], M. Marinangeli[49], J. Marks[17], A.M. Marshall[54], P.J. Marshall[60], G. Martelli[78], G. Martellotti[30], L. Martinazzoli[48,j], M. Martinelli[26,j], D. Martinez Santos[46], F. Martinez Vidal[47], A. Massafferri[1], M. Materok[14], R. Matev[48], A. Mathad[50], Z. Mathe[48], V. Matiunin[41], C. Matteuzzi[26], K.R. Mattioli[87], A. Mauri[32], E. Maurice[12], J. Mauricio[45], M. Mazurek[48], M. McCann[61], L. Mcconnell[18], T.H. Mcgrath[62], N.T. Mchugh[59], A. McNab[62], R. McNulty[18], J.V. Mead[60], B. Meadows[65], G. Meier[15], N. Meinert[76], D. Melnychuk[36],

S. Meloni[26,j], M. Merk[32,80], A. Merli[25,i], L. Meyer Garcia[2], M. Mikhasenko[48], D.A. Milanes[74], E. Millard[56], M. Milovanovic[48], M.-N. Minard[8], A. Minotti[26,j], L. Minzoni[21,f], S.E. Mitchell[58], B. Mitreska[62], D.S. Mitzel[48], A. Mödden [15], R.A. Mohammed[63], R.D. Moise[61], T. Mombächer[46], I.A. Monroy[74], S. Monteil[9], M. Morandin[28], G. Morello[23], M.J. Morello[29,m], J. Moron[34], A.B. Morris[75], A.G. Morris[56], R. Mountain[68], H. Mu[3], F. Muheim[58,48], M. Mulder[48], D. Müller[48], K. Müller[50], C.H. Murphy[63], D. Murray[62], P. Muzzetto[27,48], P. Naik[54], T. Nakada[49], R. Nandakumar[57], T. Nanut[49], I. Nasteva[2], M. Needham[58], I. Neri[21], N. Neri[25,i], S. Neubert[75], N. Neufeld[48], R. Newcombe[61], T.D. Nguyen[49], C. Nguyen-Mau[49,w], E.M. Niel[11], S. Nieswand[14], N. Nikitin[40], N.S. Nolte[64], C. Normand[8], C. Nunez[87], A. Oblakowska-Mucha[34], V. Obraztsov[44], T. Oeser[14], D.P. O'Hanlon[54], S. Okamura[21], R. Oldeman[27,e], F. Oliva[58], M.E. Olivares[68], C.J.G. Onderwater[79], R.H. O'Neil[58], A. Ossowska[35], J.M. Otalora Goicochea[2], T. Ovsiannikova[41], P. Owen[50], A. Oyanguren[47], K.O. Padeken[75], B. Pagare[56], P.R. Pais[48], T. Pajero[63], A. Palano[19], M. Palutan[23], Y. Pan[62], G. Panshin[84], A. Papanestis[57], M. Pappagallo[19,c], L.L. Pappalardo[21,f], C. Pappenheimer[65], W. Parker[66], C. Parkes[62], B. Passalacqua[21], G. Passaleva[22], A. Pastore[19], M. Patel[61], C. Patrignani[20,d], C.J. Pawley[80], A. Pearce[48], A. Pellegrino[32], M. Pepe Altarelli[48], S. Perazzini[20], D. Pereima[41], A. Pereiro Castro[46], P. Perret[9], M. Petric[59,48], K. Petridis[54], A. Petrolini[24,h], A. Petrov[81], S. Petrucci[58], M. Petruzzo[25], T.T.H. Pham[68], A. Philippov[42], L. Pica[29,m], M. Piccini[78], B. Pietrzyk[8], G. Pietrzyk[49], M. Pili[63], D. Pinci[30], F. Pisani[48], M. Pizzichemi[26,48,j], Resmi P.K[10], V. Placinta[37], J. Plews[53], M. Plo Casasus[46], F. Polci[13], M. Poli Lener[23], M. Poliakova[68], A. Poluektov[10], N. Polukhina[83,u], I. Polyakov[68], E. Polycarpo[2], S. Ponce[48], D. Popov[6,48], S. Popov[42], S. Poslavskii[44], K. Prasanth[35], L. Promberger[48], C. Prouve[46], V. Pugatch[52], V. Puill[11], H. Pullen[63], G. Punzi[29,n], H. Qi[3], W. Qian[6], J. Qin[6], N. Qin[3], R. Quagliani[49], B. Quintana[8], N.V. Raab[18], R.I. Rabadan Trejo[6], B. Rachwal[34], J.H. Rademacker[54], M. Rama[29], M. Ramos Pernas[56], M.S. Rangel[2], F. Ratnikov[42,82], G. Raven[33], M. Reboud[8], F. Redi[49], F. Reiss[62], C. Remon Alepuz[47], Z. Ren[3], V. Renaudin[63], R. Ribatti[29], S. Ricciardi[57], K. Rinnert[60], P. Robbe[11], G. Robertson[58], A.B. Rodrigues[49], E. Rodrigues[60], J.A. Rodriguez Lopez[74], E.R.R. Rodriguez Rodriguez[46], A. Rollings[63], P. Roloff[48], V. Romanovskiy[44], M. Romero Lamas[46], A. Romero Vidal[46], J.D. Roth[87], M. Rotondo[23], M.S. Rudolph[68], T. Ruf[48], R.A. Ruiz Fernandez[46], J. Ruiz Vidal[47], A. Ryzhikov[82], J. Ryzka[34], J.J. Saborido Silva[46], N. Sagidova[38], N. Sahoo[56], B. Saitta[27,e], M. Salomoni[48], C. Sanchez Gras[32], R. Santacesaria[30], C. Santamarina Rios[46], M. Santimaria[23], E. Santovetti[31,p], D. Saranin[83], G. Sarpis[14], M. Sarpis[75], A. Sarti[30], C. Satriano[30,o], A. Satta[31], M. Saur[15], D. Savrina[41,40], H. Sazak[9], L.G. Scantlebury Smead[63], A. Scarabotto[13], S. Schael[14], S. Scherl[60], M. Schiller[59], H. Schindler[48], M. Schmelling[16], B. Schmidt[48], S. Schmitt[14], O. Schneider[49], A. Schopper[48], M. Schubiger[32], S. Schulte[49], M.H. Schune[11], R. Schwemmer[48], B. Sciascia[23,48], S. Sellam[46], A. Semennikov[41], M. Senghi Soares[33], A. Sergi[24,h], N. Serra[50], L. Sestini[28], A. Seuthe[15], Y. Shang[5], D.M. Shangase[87], M. Shapkin[44], I. Shchemerov[83], L. Shchutska[49], T. Shears[60], L. Shekhtman[43,v], Z. Shen[5], V. Shevchenko[81], E.B. Shields[26,j], Y. Shimizu[11], E. Shmanin[83], J.D. Shupperd[68], B.G. Siddi[21], R. Silva Coutinho[50], G. Simi[28], S. Simone[19,c], N. Skidmore[62], T. Skwarnicki[68], M.W. Slater[53], I. Slazyk[21,f], J.C. Smallwood[63], J.G. Smeaton[55], A. Smetkina[41], E. Smith[50], M. Smith[61], A. Snoch[32], M. Soares[20], L. Soares Lavra[9], M.D. Sokoloff[65], F.J.P. Soler[59], A. Solovev[38], I. Solovyev[38], F.L. Souza De Almeida[2], B. Souza De Paula[2], B. Spaan[15], E. Spadaro Norella[25,i], P. Spradlin[59], F. Stagni[48], M. Stahl[65], S. Stahl[48], S. Stanislaus[63], O. Steinkamp[50,83], O. Stenyakin[44], H. Stevens[15], S. Stone[68], M. Straticiuc[37], D. Strekalina[83], F. Suljik[63], J. Sun[27], L. Sun[73], Y. Sun[66], P. Svihra[62], P.N. Swallow[53], K. Swientek[34], A. Szabelski[36], T. Szumlak[34], M. Szymanski[48], S. Taneja[62], A.R. Tanner[54], M.D. Tat[63], A. Terentev[83], F. Teubert[48], E. Thomas[48], D.J.D. Thompson[53], K.A. Thomson[60], V. Tisserand[9], S. T'Jampens[8], M. Tobin[4], L. Tomassetti[21,f], X. Tong[5], D. Torres Machado[1], D.Y. Tou[13], M.T. Tran[49], E. Trifonova[83],

C. Trippl[49], G. Tuci[6], A. Tully[49], N. Tuning[32,48], A. Ukleja[36], D.J. Unverzagt[17], E. Ursov[83], A. Usachov[32], A. Ustyuzhanin[42,82], U. Uwer[17], A. Vagner[84], V. Vagnoni[20], A. Valassi[48], G. Valenti[20], N. Valls Canudas[85], M. van Beuzekom[32], M. Van Dijk[49], E. van Herwijnen[83], C.B. Van Hulse[18], M. van Veghel[79], R. Vazquez Gomez[45], P. Vazquez Regueiro[46], C. Vázquez Sierra[48], S. Vecchi[21], J.J. Velthuis[54], M. Veltri[22,r], A. Venkateswaran[68], M. Veronesi[32], M. Vesterinen[56], D. Vieira[65], M. Vieites Diaz[49], H. Viemann[76], X. Vilasis-Cardona[85], E. Vilella Figueras[60], A. Villa[20], P. Vincent[13], F.C. Volle[11], D. Vom Bruch[10], A. Vorobyev[38], V. Vorobyev[43,v], N. Voropaev[38], K. Vos[80], R. Waldi[17], J. Walsh[29], C. Wang[17], J. Wang[5], J. Wang[4], J. Wang[3], J. Wang[73], M. Wang[3], R. Wang[54], Y. Wang[7], Z. Wang[50], Z. Wang[3], Z. Wang[6], J.A. Ward[56,69], N.K. Watson[53], S.G. Weber[13], D. Websdale[61], C. Weisser[64], B.D.C. Westhenry[54], D.J. White[62], M. Whitehead[54], A.R. Wiederhold[56], D. Wiedner[15], G. Wilkinson[63], M. Wilkinson[68], I. Williams[55], M. Williams[64], M.R.J. Williams[58], F.F. Wilson[57], W. Wislicki[36], M. Witek[35], L. Witola[17], G. Wormser[11], S.A. Wotton[55], H. Wu[68], K. Wyllie[48], Z. Xiang[6], D. Xiao[7], Y. Xie[7], A. Xu[5], J. Xu[6], L. Xu[3], M. Xu[7], Q. Xu[6], Z. Xu[5], Z. Xu[6], D. Yang[3], S. Yang[6], Y. Yang[6], Z. Yang[5], Z. Yang[66], Y. Yao[68], L.E. Yeomans[60], H. Yin[7], J. Yu[71], X. Yuan[68], O. Yushchenko[44], E. Zaffaroni[49], M. Zavertyaev[16,u], M. Zdybal[35], O. Zenaiev[48], M. Zeng[3], D. Zhang[7], L. Zhang[3], S. Zhang[71], S. Zhang[5], Y. Zhang[5], Y. Zhang[63], A. Zharkova[83], A. Zhelezov[17], Y. Zheng[6], T. Zhou[5], X. Zhou[6], Y. Zhou[6], V. Zhovkovska[11], X. Zhu[3], X. Zhu[7], Z. Zhu[6], V. Zhukov[14,40], J.B. Zonneveld[58], Q. Zou[4], S. Zucchelli[20,d], D. Zuliani[28], G. Zunica[62].

[1] *Centro Brasileiro de Pesquisas Físicas (CBPF), Rio de Janeiro, Brazil*
[2] *Universidade Federal do Rio de Janeiro (UFRJ), Rio de Janeiro, Brazil*
[3] *Center for High Energy Physics, Tsinghua University, Beijing, China*
[4] *Institute Of High Energy Physics (IHEP), Beijing, China*
[5] *School of Physics State Key Laboratory of Nuclear Physics and Technology, Peking University, Beijing, China*
[6] *University of Chinese Academy of Sciences, Beijing, China*
[7] *Institute of Particle Physics, Central China Normal University, Wuhan, Hubei, China*
[8] *Univ. Savoie Mont Blanc, CNRS, IN2P3-LAPP, Annecy, France*
[9] *Université Clermont Auvergne, CNRS/IN2P3, LPC, Clermont-Ferrand, France*
[10] *Aix Marseille Univ, CNRS/IN2P3, CPPM, Marseille, France*
[11] *Université Paris-Saclay, CNRS/IN2P3, IJCLab, Orsay, France*
[12] *Laboratoire Leprince-Ringuet, CNRS/IN2P3, Ecole Polytechnique, Institut Polytechnique de Paris, Palaiseau, France*
[13] *LPNHE, Sorbonne Université, Paris Diderot Sorbonne Paris Cité, CNRS/IN2P3, Paris, France*
[14] *I. Physikalisches Institut, RWTH Aachen University, Aachen, Germany*
[15] *Fakultät Physik, Technische Universität Dortmund, Dortmund, Germany*
[16] *Max-Planck-Institut für Kernphysik (MPIK), Heidelberg, Germany*
[17] *Physikalisches Institut, Ruprecht-Karls-Universität Heidelberg, Heidelberg, Germany*
[18] *School of Physics, University College Dublin, Dublin, Ireland*
[19] *INFN Sezione di Bari, Bari, Italy*
[20] *INFN Sezione di Bologna, Bologna, Italy*
[21] *INFN Sezione di Ferrara, Ferrara, Italy*
[22] *INFN Sezione di Firenze, Firenze, Italy*
[23] *INFN Laboratori Nazionali di Frascati, Frascati, Italy*
[24] *INFN Sezione di Genova, Genova, Italy*
[25] *INFN Sezione di Milano, Milano, Italy*
[26] *INFN Sezione di Milano-Bicocca, Milano, Italy*
[27] *INFN Sezione di Cagliari, Monserrato, Italy*
[28] *Universita degli Studi di Padova, Universita e INFN, Padova, Padova, Italy*
[29] *INFN Sezione di Pisa, Pisa, Italy*
[30] *INFN Sezione di Roma La Sapienza, Roma, Italy*
[31] *INFN Sezione di Roma Tor Vergata, Roma, Italy*

[32] *Nikhef National Institute for Subatomic Physics, Amsterdam, Netherlands*
[33] *Nikhef National Institute for Subatomic Physics and VU University Amsterdam, Amsterdam, Netherlands*
[34] *AGH - University of Science and Technology, Faculty of Physics and Applied Computer Science, Kraków, Poland*
[35] *Henryk Niewodniczanski Institute of Nuclear Physics Polish Academy of Sciences, Kraków, Poland*
[36] *National Center for Nuclear Research (NCBJ), Warsaw, Poland*
[37] *Horia Hulubei National Institute of Physics and Nuclear Engineering, Bucharest-Magurele, Romania*
[38] *Petersburg Nuclear Physics Institute NRC Kurchatov Institute (PNPI NRC KI), Gatchina, Russia*
[39] *Institute for Nuclear Research of the Russian Academy of Sciences (INR RAS), Moscow, Russia*
[40] *Institute of Nuclear Physics, Moscow State University (SINP MSU), Moscow, Russia*
[41] *Institute of Theoretical and Experimental Physics NRC Kurchatov Institute (ITEP NRC KI), Moscow, Russia*
[42] *Yandex School of Data Analysis, Moscow, Russia*
[43] *Budker Institute of Nuclear Physics (SB RAS), Novosibirsk, Russia*
[44] *Institute for High Energy Physics NRC Kurchatov Institute (IHEP NRC KI), Protvino, Russia, Protvino, Russia*
[45] *ICCUB, Universitat de Barcelona, Barcelona, Spain*
[46] *Instituto Galego de Física de Altas Enerxías (IGFAE), Universidade de Santiago de Compostela, Santiago de Compostela, Spain*
[47] *Instituto de Fisica Corpuscular, Centro Mixto Universidad de Valencia - CSIC, Valencia, Spain*
[48] *European Organization for Nuclear Research (CERN), Geneva, Switzerland*
[49] *Institute of Physics, Ecole Polytechnique Fédérale de Lausanne (EPFL), Lausanne, Switzerland*
[50] *Physik-Institut, Universität Zürich, Zürich, Switzerland*
[51] *NSC Kharkiv Institute of Physics and Technology (NSC KIPT), Kharkiv, Ukraine*
[52] *Institute for Nuclear Research of the National Academy of Sciences (KINR), Kyiv, Ukraine*
[53] *University of Birmingham, Birmingham, United Kingdom*
[54] *H.H. Wills Physics Laboratory, University of Bristol, Bristol, United Kingdom*
[55] *Cavendish Laboratory, University of Cambridge, Cambridge, United Kingdom*
[56] *Department of Physics, University of Warwick, Coventry, United Kingdom*
[57] *STFC Rutherford Appleton Laboratory, Didcot, United Kingdom*
[58] *School of Physics and Astronomy, University of Edinburgh, Edinburgh, United Kingdom*
[59] *School of Physics and Astronomy, University of Glasgow, Glasgow, United Kingdom*
[60] *Oliver Lodge Laboratory, University of Liverpool, Liverpool, United Kingdom*
[61] *Imperial College London, London, United Kingdom*
[62] *Department of Physics and Astronomy, University of Manchester, Manchester, United Kingdom*
[63] *Department of Physics, University of Oxford, Oxford, United Kingdom*
[64] *Massachusetts Institute of Technology, Cambridge, MA, United States*
[65] *University of Cincinnati, Cincinnati, OH, United States*
[66] *University of Maryland, College Park, MD, United States*
[67] *Los Alamos National Laboratory (LANL), Los Alamos, United States*
[68] *Syracuse University, Syracuse, NY, United States*
[69] *School of Physics and Astronomy, Monash University, Melbourne, Australia, associated to* [56]
[70] *Pontifícia Universidade Católica do Rio de Janeiro (PUC-Rio), Rio de Janeiro, Brazil, associated to* [2]
[71] *Physics and Micro Electronic College, Hunan University, Changsha City, China, associated to* [7]
[72] *Guangdong Provincial Key Laboratory of Nuclear Science, Guangdong-Hong Kong Joint Laboratory of Quantum Matter, Institute of Quantum Matter, South China Normal University, Guangzhou, China, associated to* [3]
[73] *School of Physics and Technology, Wuhan University, Wuhan, China, associated to* [3]
[74] *Departamento de Fisica , Universidad Nacional de Colombia, Bogota, Colombia, associated to* [13]
[75] *Universität Bonn - Helmholtz-Institut für Strahlen und Kernphysik, Bonn, Germany, associated to* [17]
[76] *Institut für Physik, Universität Rostock, Rostock, Germany, associated to* [17]
[77] *Eotvos Lorand University, Budapest, Hungary, associated to* [48]
[78] *INFN Sezione di Perugia, Perugia, Italy, associated to* [21]
[79] *Van Swinderen Institute, University of Groningen, Groningen, Netherlands, associated to* [32]
[80] *Universiteit Maastricht, Maastricht, Netherlands, associated to* [32]

[81] National Research Centre Kurchatov Institute, Moscow, Russia, associated to [41]
[82] National Research University Higher School of Economics, Moscow, Russia, associated to [42]
[83] National University of Science and Technology "MISIS", Moscow, Russia, associated to [41]
[84] National Research Tomsk Polytechnic University, Tomsk, Russia, associated to [41]
[85] DS4DS, La Salle, Universitat Ramon Llull, Barcelona, Spain, associated to [45]
[86] Department of Physics and Astronomy, Uppsala University, Uppsala, Sweden, associated to [59]
[87] University of Michigan, Ann Arbor, United States, associated to [68]

[a] Universidade Federal do Triângulo Mineiro (UFTM), Uberaba-MG, Brazil
[b] Hangzhou Institute for Advanced Study, UCAS, Hangzhou, China
[c] Università di Bari, Bari, Italy
[d] Università di Bologna, Bologna, Italy
[e] Università di Cagliari, Cagliari, Italy
[f] Università di Ferrara, Ferrara, Italy
[g] Università di Firenze, Firenze, Italy
[h] Università di Genova, Genova, Italy
[i] Università degli Studi di Milano, Milano, Italy
[j] Università di Milano Bicocca, Milano, Italy
[k] Università di Modena e Reggio Emilia, Modena, Italy
[l] Università di Padova, Padova, Italy
[m] Scuola Normale Superiore, Pisa, Italy
[n] Università di Pisa, Pisa, Italy
[o] Università della Basilicata, Potenza, Italy
[p] Università di Roma Tor Vergata, Roma, Italy
[q] Università di Siena, Siena, Italy
[r] Università di Urbino, Urbino, Italy
[s] MSU - Iligan Institute of Technology (MSU-IIT), Iligan, Philippines
[t] AGH - University of Science and Technology, Faculty of Computer Science, Electronics and Telecommunications, Kraków, Poland
[u] P.N. Lebedev Physical Institute, Russian Academy of Science (LPI RAS), Moscow, Russia
[v] Novosibirsk State University, Novosibirsk, Russia
[w] Hanoi University of Science, Hanoi, Vietnam